Effect of physical aging on scratch behavior of polycarbonate

L. De Noni[1,2], X. Zhu[1], L. Andena[2], K. Noh[1], Y. Li[3], P. Vollenberg[3] and H.-J. Sue[1,*]

[1]Polymer Technology Center, Department of Materials Science Engineering, Texas A&M University, College Station, TX 77843-3123, US

[2]Dipartimento di Chimica, materiali e ingegneria chimica “G. Natta", Politecnico di Milano, Milan, Italy

[3]SABIC’s Specialties business, Mount Vernon, IN, US

* Corresponding author:

Hung-Jue Sue
Polymer Technology Center, Department of Materials Science Engineering
Texas A&M University, 575 Ross Street
College Station, TX 77843-3123, US

E-mail: hjsue@tamu.edu

Abstract

Physical aging refers to relaxation of the polymer glassy state toward the amorphous state and this phenomenon affects their physical-mechanical properties. This work investigates the effect of physical aging on polymer scratch behavior and visibility. It was shown that mechanical properties were significantly modified over the aging time, especially the yield stress, in turn affecting polymer scratch behavior. As a matter of fact, the critical load for the onset of scratch visibility was shown to increase with the aging, thus improving sensitivity of polymer to scratches. Such behavior was strictly related to the yield stress increase with the aging time. The usefulness of the present work is highlighted, and some future perspectives are discussed.

Highlights

- The influence of physical aging on the mechanical behavior of polymers, in particular yield stress, was quantified;
- Scratch behavior and visibility are also affected by aging, with the polymer becoming less sensitive to scratch damage over time;
- A quantitative determination based on the increase of the critical load for the onset of visibility was reported;
- A general relationship between critical load for visibility and yield stress for polycarbonate was proposed.

1. Introduction

Polymer scratch behavior has been widely studied during the past three decades [1–27]. Scratch behavior has been related to polymer mechanical behavior [1, 2, 5–8, 14, 16, 26, 28–30] such as modulus [1], yield stress [2, 14], and strain hardening [5, 12], which can significantly affect polymer scratch behavior. Also, any chemical or physical phenomenon that modifies the mechanical behavior of polymers, such as chemical oxidation [21, 23, 31] and physical aging [15], can have an impact on scratch response. While strategies exist to prevent chemical oxidation, physical ageing is an inherent phenomenon occurring in plastic products after processing; increasing the service life of polymers in automotive, electrical appliances, household goods, and other decorative applications then requires an assessment of their scratch behavior after prolonged physical aging.

Physical aging is a unique phenomenon for polymers, which can occur in absence of externally applied loads, at constant temperature, and without alterations of the material structure, i.e., no chemical degradation taking place [31–34]. It is called "*aging"* because this phenomenon leads over time to a change in the properties of the materials, such as density, modulus, yield stress, etc. These properties are commonly utilized as a marker of the occurrence of an aging process. It is a reversible phenomenon since no chemical change occurs, and the initial properties can be restored upon heating the material above its glass transition temperature. The driving force for physical aging is induced by the natural tendency of non-equilibrium state to move toward the equilibrium state, i.e., a relaxation process of the glassy state. The origin of this phenomenon is largely driven by the fabrication process of thermoplastics. For instance, injection molded components are cooled down below the glass transition temperature (T_g) quickly, with a cooling rate that does not allow the polymeric chains to have enough time to reach a minimum energy configuration: consequently, the structure is frozen into a non-equilibrium state condition. This is shown in Figure 1 by the solid line, while the dotted line instead represents the ideal equilibrium condition. These materials must be intended as solidified supercooled liquids, whose volume, enthalpy, and entropy are greater than they would have been in an equilibrium state.

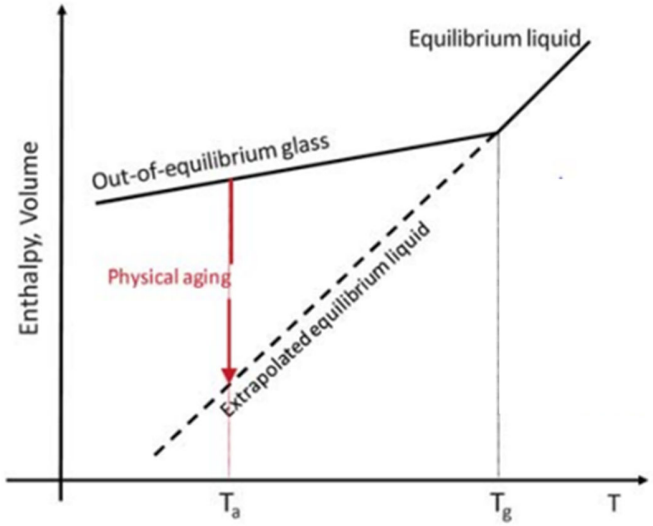

Figure 1. Schematic picture describing the origin of the aging phenomenon: the aging temperature range is shown below the glass transition temperature [36].

While transition towards equilibrium is kinetically inhibited, some degree of molecular mobility exists even below the glass transition temperature and molecular relaxation phenomena can still take place, bringing the system closer to equilibrium. This slow process modifies the time-dependent properties in the glassy state, as the molecular chains become more densely packed. The material becomes stiffer and more brittle, and its molecular mobility decreases; the same happens for the creep and the relaxation rates and the dielectric constant. This phenomenon is usually explained in the most straightforward and qualitative way by the free volume theory [37]. The rate of this phenomenon depends on the distance from the glass transition temperature: the process is faster as the aging temperature approaches the polymer glass transition. The aging progression can usually be quantified and measured through calorimetric analysis or mechanical tests. Specifically, this process exhibits an endothermic peak, usually named "*excess enthalpy*". This was demonstrated in several studies [37–40]. As mentioned, the physical aging also modifies the mechanical performances of the materials [5, 31, 32, 34, 41–44], as shown in Figure 2 for polystyrene samples where an increase in elastic modulus and strength is observed because of the reduced molecular mobility over the aging time; the effect on yielding is also visible in Figure 3 for an epoxy resin. Widely available data for bisphenol-A polycarbonate (PC) [45–55] demonstrates that aging induces an increase in the modulus and the yield stress and a reduction of the strain at break, until the material experiences a ductile-to-brittle transition after extended aging periods (over 300 h) at 120 °C (i.e., about 30°C lower than T_g).

The effect of these changes on the mechanical properties certainly affects the scratch behavior, too [56,57]. However, to the best of our knowledge, there exist very few studies dealing with the scratch behavior of physically-aged polycarbonate (PC) [58]. The aim of the present research is to investigate the effect of physical aging on the scratch behavior of PC. This is of relevance for a couple of reasons: first, all polymeric materials are more or less subjected to this phenomenon, even for applications at room temperature. Secondly, it is helpful for the understanding and the identification of a general relationship between the mechanical properties and the scratch response. As a matter of fact, the mechanical behavior is modified over the aging time, and consequently the scratch response. To do so, the aim is to quantify the progression of the aging phenomenon and to evaluate how this affects scratch performance from a mechanical point of view, also in terms of polymer deformation processes that lead to scratch visibility.

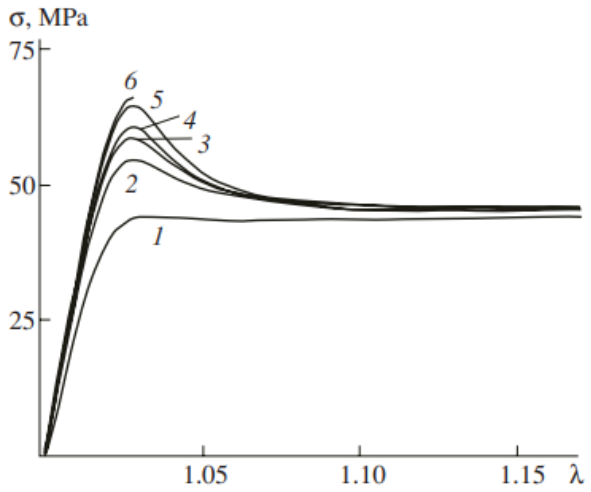

Figure 2. Effect of physical aging on the uniaxial tensile stress-strain curves for polystyrene samples at different aging time: 1) 1 minute; 2) 0.5 hour; 3) 1 hour; 4) 5 hours: 5) 19 hours and 6) 48 hours [58–60].

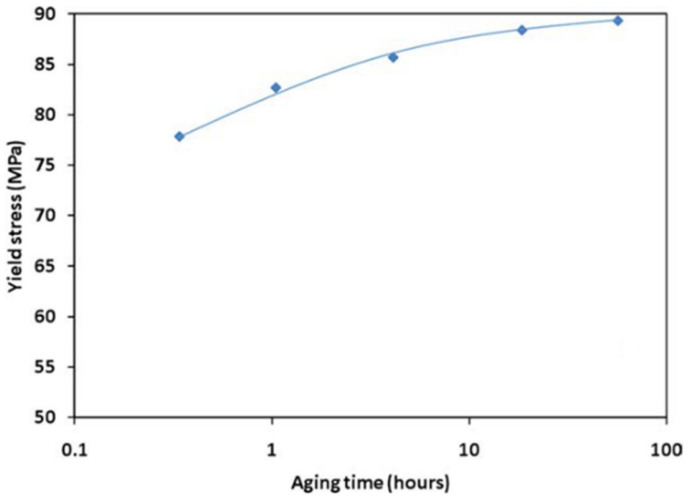

Figure 3. The effect of physical aging on the mechanical behavior, specifically yielding, of epoxy polymers (and their composites). The figure shows the increase of the yield stress with the aging time [20].

2. Experimental section

2.1 Materials and methods

Black injection molded glossy samples made of bisphenol A PC and of a bisphenol A, cyclohexylidene-bridged bisphenol PC copolymer (CoPC) were supplied by SABIC's Specialties business in the form of rectangular plaques with dimensions of 100.0 mm × 100.0 mm × 3.2 mm for the scratch tests. Dog-bone shaped and prismatic samples were also manufactured for the tensile and compression tests, respectively. These samples were utilized to evaluate the effect of physical aging on scratch behavior.

2.2 Aging protocol

The samples were subjected to a conditioning step, consisting of a thermal treatment at 160 °C (above the glass transition temperature T_g of all tested samples). The aim of the treatment is to erase the previous thermal history related to the manufacturing process. To do so, samples were put into a ventilated oven at 160 °C for 30 minutes. They were subsequently removed and slowly cooled under forced air down to room temperature. Even a very slow cooling rate can only freeze the chains in a partially liquid-like, high free volume non-equilibrium state. For such a reason, an arbitrary aging time of 1h was attributed to the samples following this heat treatment.

The aging treatment was conducted at 120 °C in a ventilated oven for 80, 160, 300 and 460 hours, respectively. The same aging temperature was selected for the two materials, so that a single oven could be used for both sets of samples. It was chosen so that its value is relatively close to T_g, to facilitate molecular movements which bring the polymer closer to the equilibrium state. These samples underwent tension/compression mechanical testing, FTIR and GPC analysis, DSC analysis and scratch tests.

2.3 Scratch test

Scratch tests were performed utilizing a Surface Machine Systems instrument (Austin, TX). The machine was equipped with normal and tangential load cells of 200 N capacity. A linearly increasing normal load was applied from 1 to 130 N. A spherical indenter (1 mm diameter) made of stainless steel was slid at 100 mm/s velocity for 80 mm (scratch length). The apparent scratch coefficient of friction was determined as per Equation 1:

$$SCOF = \frac{F_t}{F_n} \qquad \text{(Eq. 1)}$$

where F_n [N] and F_t [N] are the normal and tangential load, respectively. At least 4 scratches per aging time sample were performed. Only the average curves are shown as the data are quite reproducible (within 10% for the tangential force F_t).

2.4 Tensile and compression tests

Tensile and compression tests were performed to quantify the mechanical response of PC and CoPC over the aging time. Uniaxial quasi-static tensile tests were performed on an Instron 5967 screw-driven dynamometer equipped with a 10 kN load cell. Compression tests were carried out using an Instron 1185R5800 dynamometer equipped with 100kN load cell fitted with compression plates at constant crosshead speeds that was used to provide the strain rate imposed during the tests (for either tensile and compression tests). Dog-bone shaped samples with dimensions of 12.75 mm × 3.20 mm and a gauge length of 70 mm were injection molded for the tensile test. Square prismatic samples with a 12.5 mm × 12.5 mm cross-section and height 6.0 mm were cut from injection molded bar shaped samples. The applied nominal strain rate was 0.006 s^{-1} in both cases and it was controlled through the crosshead displacement. The actual strain was measured using a clip-gauge extensometer placed on the gauge length of tensile samples or between the compression plates. Three samples per material and aging time were tested.

2.5 Confocal laser microscope analysis

A high-resolution Keyence VK9700 violet laser scanning confocal microscope (VLSCM) was used to analyze the scratch deformation and measure the scratch geometry for the materials under investigation (for each scratch). Scratches were investigated 24 hours after performing scratch tests. The same procedure was applied for all tested materials. Time was selected to allow a complete recovery of the viscoelastic component of scratch deformation.

2.6 Differential scanning calorimetry analysis

DSC was performed using a TA Q20 instrument. In this work, the aging behavior of PC samples was studied. Therefore, DSC analysis was meant to measure the main thermal transitions for the unaged PC and to quantify the progression of the aging phenomenon. The selected heating history for the DSC analysis is:

a) First heating ramp: from 40 to 180 °C, applying a heating rate of 10 °C/min;
b) Cooling ramp: from 180 °C to 40 °C, with a cooling rate of 10 °C/min;
c) Second heating ramp: from 40 °C to 180 °C with a heating rate of 10 °C/min.

The excess enthalpy, related to the aging phenomenon, was quantified [38, 46] as described in Figure 4, by measuring the area below the endothermal peak according to the method described in [38, 46]:

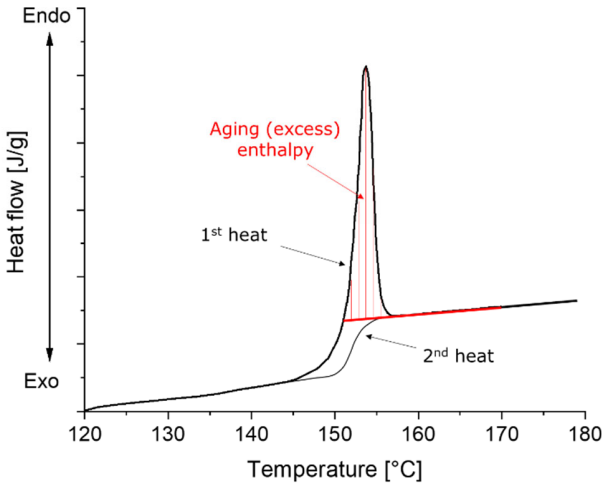

Figure 4. Schematic description of the methodology applied for the measurement of the enthalpy peak related to the aging phenomenon during the first heating: area below the endothermic peak where the straight red line represents the baseline of the area. The procedure was consistently employed for all tested samples. The second heating ramp is also shown in the picture: it shows the glass transition at the same location of the pristine sample as the phenomenon is reversible upon heating above the material T_g) [50].

The first step is the determination of the glass transition temperature of the unaged PC. In this sense, the first heating ramp was meant to erase the previous thermal history. The second heating ramp aims at determining the actual glass transition temperature of the tested samples. As a matter of fact, PC samples show a higher glass transition temperature (149 °C) compared to the CoPC material (142 °C), as described in Figure 5. It is also worth noticing (Figure 5) that the distance ΔT between the glass transition temperature (for each material) and the selected aging temperature (120 °C) differs by a few °C, i.e., the ΔT is equal to 29 °C and 22 °C for PC and CoPC, respectively. This leads to the expectation that the extent of the aging phenomenon should be larger for the CoPC, as the chosen aging temperature is closer to its glass transition.

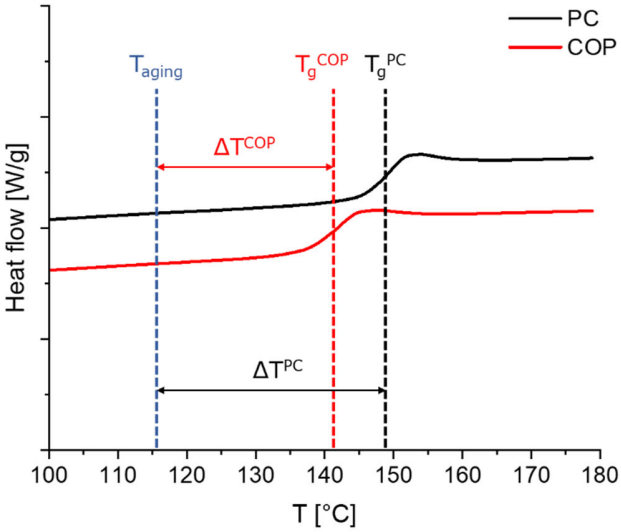

Figure 5. Determination of the glass transition temperature for PC (149 °C) and CoPC (142 °C); also, a schematic representation of the difference between the glass transition temperature and the selected aging temperature (120 °C) is reported.

The second step is the measurement of the progression of the aging phenomenon (as described in Figure 4): to do so, the first heating was considered. The second heating ramp, instead, was meant to double check that the phenomenon is reversible, i.e., physical. To be reversible, the measured glass transition temperature should overlap with the unaged glass transition. This was demonstrated for all tested samples. Only one test was carried out for each aging time study.

2.7 FTIR analysis

FTIR was carried out using a Nicolet 380 instrument in reflectance mode, in the wavenumber range from 600 to 3250 cm^{-1}. Multiple (128) scans were averaged for optimal data quality. The machine allows to qualitatively and quantitively measure the chemical composition on the surface of the sample. The samples were cut from the plaques for the scratch test and only the upper surface was analyzed as no difference was detected between the upper and bottom ones. The aim of the analysis was to check whether any chemical degradation phenomena took place during the aging procedure. The analysis was carried out for unaged and aged samples daily (after each 24 hours). However, only data for unaged and 460 hours aged samples are shown.

2.8 Gel permeation chromatography

GPC analysis was performed using Agilent 1260 equipment to study if any chemical change occurs with aging, evaluating any variation in the number-average molecular weight M_n and the weight average molecular weight M_w. The analysis was performed at the SABIC's Specialties business laboratory (Indiana, USA). Agilent PL gel Mixed-C column was used. Methylene chloride was chosen as a solvent with a solvent flow rate of 1.0 ml/min and an injection volume of 50 µl.

2.9 Black box setup and image analysis

Scratch visibility analysis was performed utilizing a black box setup [18,61,62], whose schematic picture is shown in Figure 6a below. A detailed description is given in a previous publication [24]. The settings of the camera were optimized to accurately capture all the details (i.e., the scratch surface deformation features): ISO-800, the exposure time at 1/30 s, and aperture angle of 4/5. The camera settings were

consistently used for all the tested samples. The relative orientation of the illuminant and the sample (specifically, the scratch on the sample surface) are shown in Figure 6b.

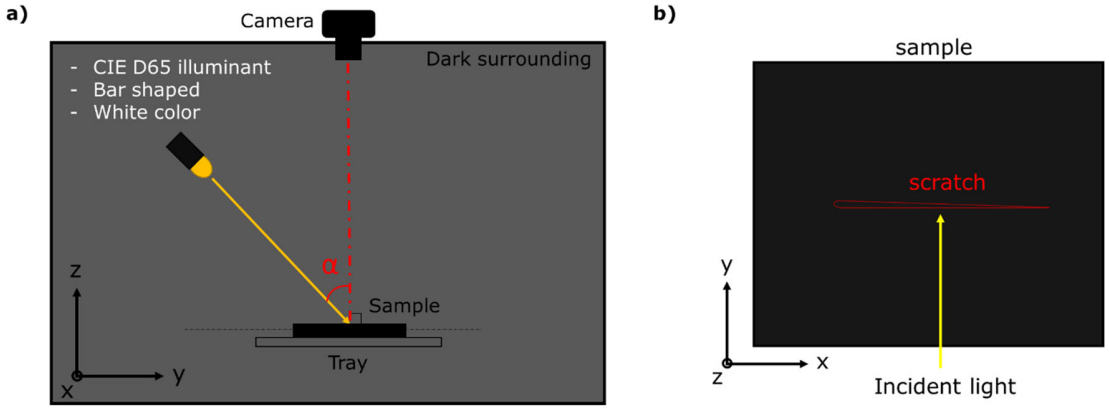

Figure 6. a) Sketch representing the custom-built black box setup. The sample is placed onto the tray and the illuminant can be rotated at a certain angle α (at a fixed distance from the samples). The camera is aligned with the normal to the surface of the samples. b) The projection of the incident light direction is perpendicular to the scratching direction.

The images were subsequently analyzed by measuring the contrast between the scratched and undamaged area. In particular, the contrast is defined according to Equation 4.2 [63], [64]:

$$C\ [\%] = \frac{I_S - I_b}{I_S + I_b} * 100 \qquad \text{(Eq. 2)}$$

where I_s is the luminance of the scratched area and I_b is the luminance of the background. The criterion requires to define the region that exceeds a certain selected contrast threshold. The minimum load where this criterion is satisfied is defined as "*critical load*" for the onset of visibility. The contrast threshold is properly selected to match the human perception of the scratch. The human eye perception is measured through a psychophysical test: the observers were properly taught how to determine the critical load for the onset of visibility. At least five observers utilized the same black box setup to determine the onset of visibility for the tested samples (the room was completely darkened).

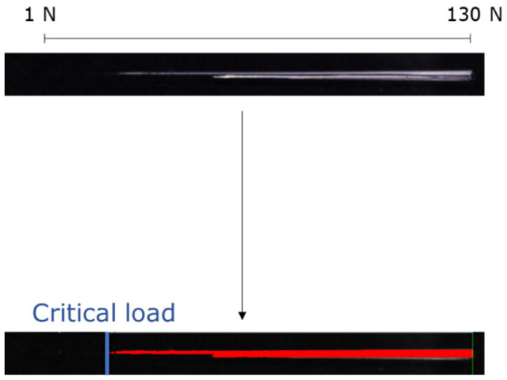

Figure 7. Schematic representation of the image analysis procedure. At the top, the image was taken with the camera in the black box; then, the image is analyzed with a software through which the user is allowed to select the contrast threshold, which results in the image at the bottom. The red area indicates the region where the contrast value exceeds the specified threshold. The critical load is defined as the minimum load that satisfies this criterium.

3. Results and discussion

The aim of the section is to provide findings for assessing the long-term behavior of PC components, trying to quantify their surface mechanical durability which is crucial when it comes to sustainability. The role of physical aging on the scratch response of the PC and CoPC samples was investigated. The discussion is divided into sub-sections to address and answer the following points:

a) Ensure that the phenomenon is physical, i.e., reversible;
b) Quantify the progression of the aging;
c) Evaluate the effect of aging on the scratch behavior and its visibility.

3.1 Possible effect of the physical aging on the polymer chemical structure

Possible changes in the chemical structure of the selected materials were monitored utilizing FTIR in reflectance mode and performing GPC analysis. The FTIR analysis shows that both spectra show the characteristics peaks of polycarbonate: C=O stretching at about 1777 cm^{-1}, O-C-O stretching at about 1230 cm^{-1} and O-C-C stretching at about 1015 cm^{-1}. FTIR spectra show no significant differences in the absorbance spectra between unaged and 460 hours aged samples as highlighted in Figure 8. It appears that no detectable chemical degradation occurs on the surface of the samples as the spectra are almost perfectly overlapped. The intensity and the position of the peaks are the same.

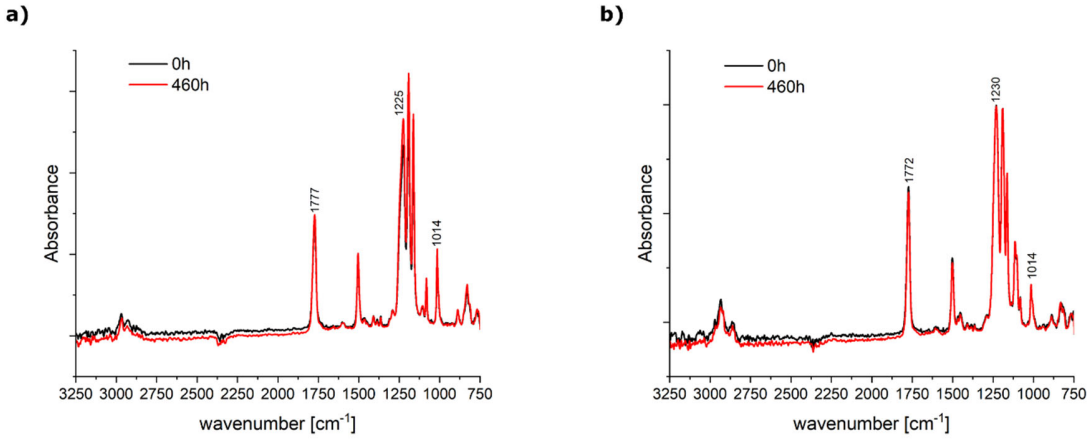

Figure 8. Absorbance spectra for a) polycarbonate (PC) and b) polycarbonate copolymer (CoPC). Characteristics peaks of polycarbonate are shown. Black curve represents the data for the unaged sample (0 hours), whereas the red curve describes the data after 460 hours aging.

To further the investigation of possible molecular weight reduction due to thermal aging, GPC analysis was carried out. The same samples used for FTIR were analyzed. The number-average molecular weight M_n and the weight average molecular weight M_w of the unaged and aged (460 hours) samples remain almost the same, as shown in Table 2-1. Even in this case, changes are negligible. This confirms that the considered aging phenomenon is a physical process that involves only reversible changes.

Table 2-1. Percentage variations [%] in the number-average molecular weight (M_n) and weight average molecular weight (M_w) between the unaged (0 hour) and 460 hours aged samples, for both PC and CoPC materials.

Δ(0 – 460 hours)	**PC**	**PC copolymer**
M_n [%]	-0.58	-0.03

M_w [%]	-0.14	-0.71

3.2 Effect of the physical aging on calorimetric properties

The quantification of the aging phenomenon was measured through DSC analysis. The approach requires the determination of the endothermic (excess) enthalpy peak associated to the aging phenomenon as described in the materials and methods section. Figure 9 below describes the progression of this variable. It is worth noticing that an increasing trend is observed for both PC and CoPC samples. This same phenomenon was also observed in several other studies [49, 52]. The trend has been found to follow a linear relationship for most systems investigated, but not for the PC system studied here. There appears to be a transition during the aging process. This interesting finding will be addressed in a future investigation. What is worth highlighting is the steadily increasing excess enthalpy with the aging time, which confirms the evolution of the aging phenomenon at the selected temperature of 120°C.

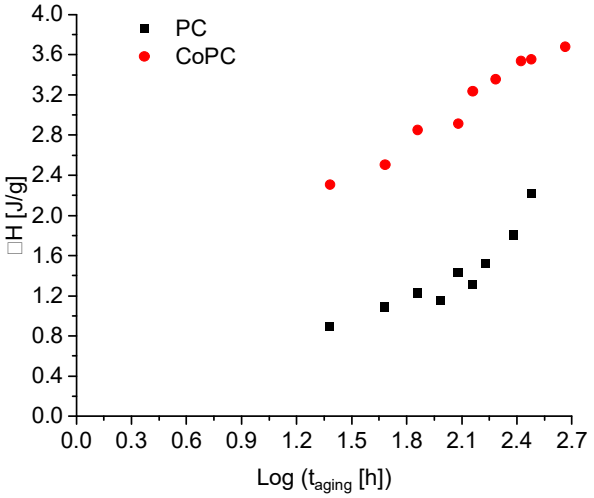

Figure 9. Increase of the excess enthalpy with the aging time (logarithmic scale) for PC and PC copolymer samples.

Its effect on the enthalpy is significantly increasing over the selected aging time up to 460 hours. The relative variation is high enough to imply that the mechanical properties must also be affected by aging. It is noted that the extent of the aging phenomenon is larger for CoPC samples, as shown by the excess enthalpy values in Figure 9. This agrees with the lower ΔT resulting for the copolymer sample. Accordingly, larger variations of the material properties may be expected for CoPC.

3.3 Effect of the physical aging on mechanical properties

It has been shown that the physical aging has an impact on the mechanical behavior of polymers [32], [33], [42], [44], [47], [50]. Specifically, PC samples undergo a transition from ductile to brittle behavior after several hours of aging at 120 °C [47]. This leads to an increase of the elastic modulus and yield stress, and a concurrent reduction of the ductility [50]. Tensile and compression tests were performed to quantify these variations in the mechanical response. Figure 10 shows the stress-strain curves for (a) PC and (b) CoPC. As shown, both materials experience an increase in the modulus and yield stress as expected, and a reduction in the strain at break. Tensile behavior has been shown to correlate well with the scratch-induced

cracks, crazing, and stress whitening right behind the scratch tip; however, compressive behavior is found to be more relevant to the plastic deformation in front and underneath the scratch tip, as shown in Figure 11 [4]. The actual stress state is obviously much more complex; however, several works showed that the scratch behavior can be well correlated to material properties, such as uniaxial compressive yield stress or tensile strength [1], [14], [26]). It should be noted that compressive yield stress measured through true stress-strain curves is the most crucial factor for polymers showing ductile ploughing [17]. The same trend is observed in the compression tests (Figure 12). The materials experience an increase in both modulus and yield stress.

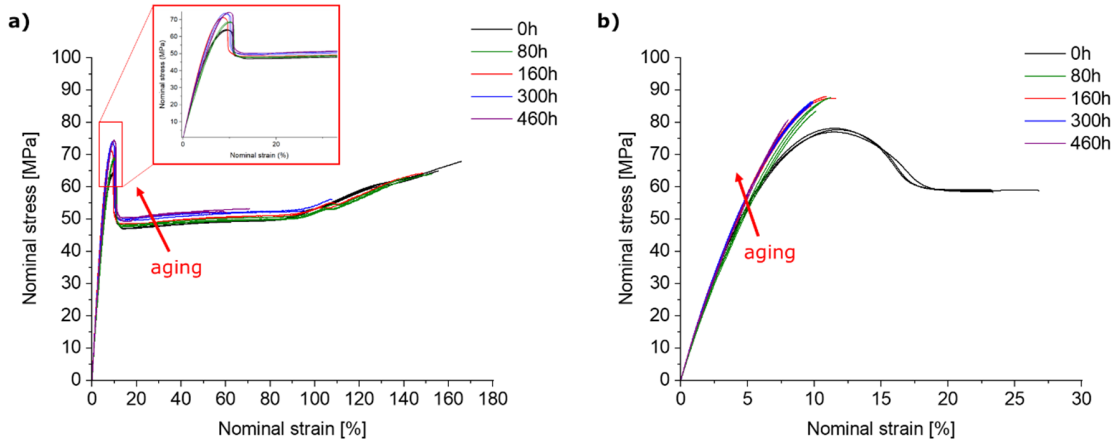

Figure 10. Nominal stress-strain curved for a) PC and b) PC copolymer obtained through tensile test. For each material, the results for unaged (black curves), 160 hours aged (red curves), 300 hours aged (blue lines) and 460 hours aged (purple lines) samples are reported.

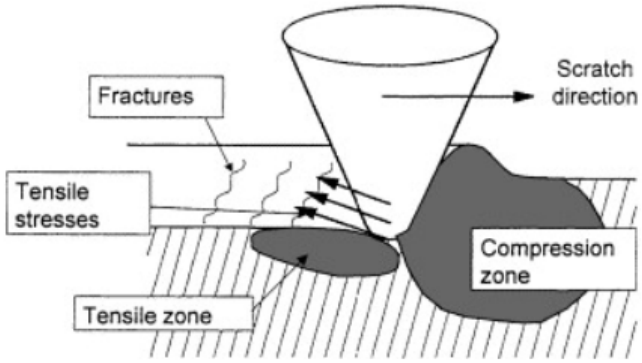

Figure 11. Schematic description of the stress state induced under scratching conditions: a region under compression in front of the indenter and a tensile zone behind it [4].

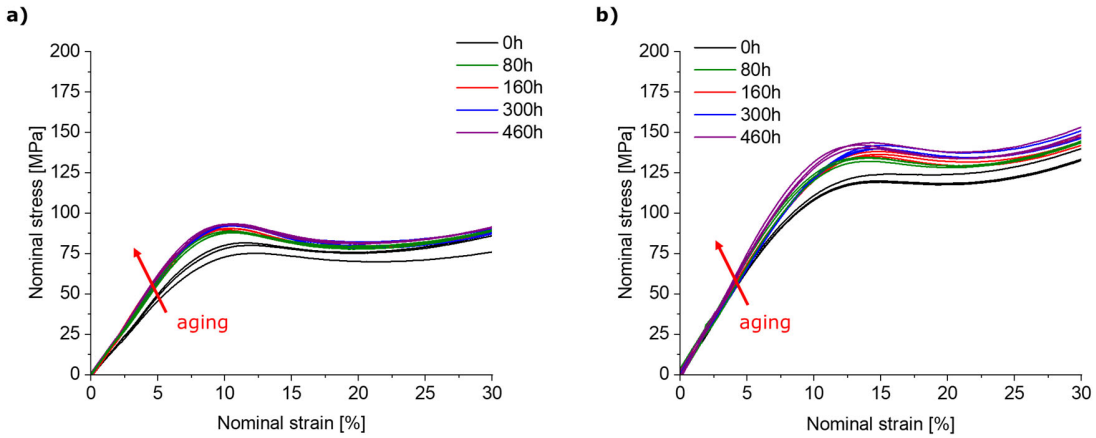

Figure 12. Nominal stress-strain curved for a) PC and b) PC copolymer obtained through compression test. For each material, the results for unaged (black curves), 160 hours aged (red curves), 300 hours aged (blue lines) and 460 hours aged (purple lines) samples are reported.

Since the mechanical behavior significantly varies, the scratch response is expected to be affected by these changes. The idea is to find a key parameter, for instance the modulus or the yield stress, able to properly correlate with the phenomenon. The selection of such parameter needs to happen according to the observed scratch deformation mechanism. As mentioned, it is shown that the compressive yield stress (measured as the maximum of the stress-strain curve) varies with the aging as described in Figure 13. Yield stress almost linearly increases with the logarithm of the aging time. This material property was shown to be a key factor for materials showing ductile ploughing [14]. In this sense, the compressive yield stress is seen as the threshold above which the plastic deformation of the material starts taking place, i.e., the material is pushed by the indenter and starts "flowing" around it.

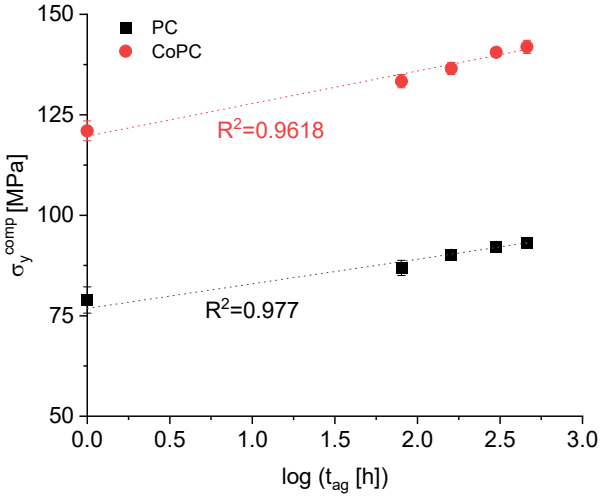

Figure 13. The variations of the compressive yield stress (measured as the maximum of the stress-strain curves) with the aging time for both PC and PC copolymer is shown. The data are represented for the unaged (0 hour), 80-, 160-, 300- and 460-hours aged samples. The graph shows the trend for the compressive yield stress vs the logarithm of the aging time.

3.4 Effect of physical aging on the scratch behavior

The scratch behavior is expected to be affected by the aging phenomenon even though there is not much literature related to PC. Figure 14a and Figure 14b show the trend of the average curve of the "apparent" scratch coefficient of friction (SCOF) for each aging time, on PC and CoPC. Data at low loads are quite noisy because of inertial effects of the machine, and for this reason the first 10 mm along the scratch length were neglected. The apparent SCOF appears to be higher for the PC samples compared to CoPC. A higher friction was shown to result in a larger susceptibility of the material to scratches, and therefore lower scratch resistance [65, 66, 67]. It also seems that the SCOF slightly decreases over the aging time in either case, at least by considering the reference unaged sample and the trend of all aged samples. In particular, for PC a significant decrease can be observed for times longer than 100h; the trend is not so clear in the case of CoPC. Therefore, any effects on the scratch behavior due to aging appears to be a consequence of the changes in the mechanical properties. This is clearly explained by stress-strain curves reported in Figure 10 and Figure 12. CoPC is characterized by higher yield stress, meaning that its scratch resistance is greater as already shown in other studies [1], [14], [26]. The scratch deformation mechanisms were investigated utilizing a confocal laser microscope. It is worth noticing that both materials show ductile ploughing first, followed by ductile ploughing + cracking as the load increases and eventually ductile ploughing + stress whitening at high load, as shown in Figure 15. Scratch deformation mechanism varies with the applied increasing normal load as shown in several works [1,2,4]. Ductile ploughing is the deformation mechanism responsible for scratch visibility for ductile polymers. However, it is worth mentioning that as the applied normal load increases, cracks formation takes place in the scratch groove as a result of tensile stresses arising beneath the indenter [4]. At higher loads, stress whitening occurs inside the scratch groove. It was already demonstrated that the compressive yield stress can dominate the scratch behavior of polymers when the observed deformation mechanism is ductile ploughing [14], [26]. This confirms that yield stress could be regarded as a dominant parameter for describing polycarbonate samples scratch response.

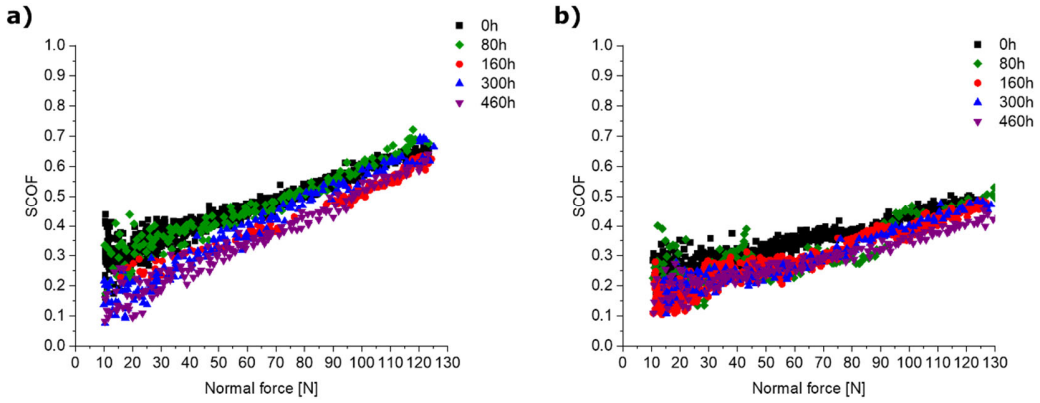

Figure 14. SCOF average curves for a) PC and b) COP for different aging time, 0, 80, 160, 300 and 460 hours.

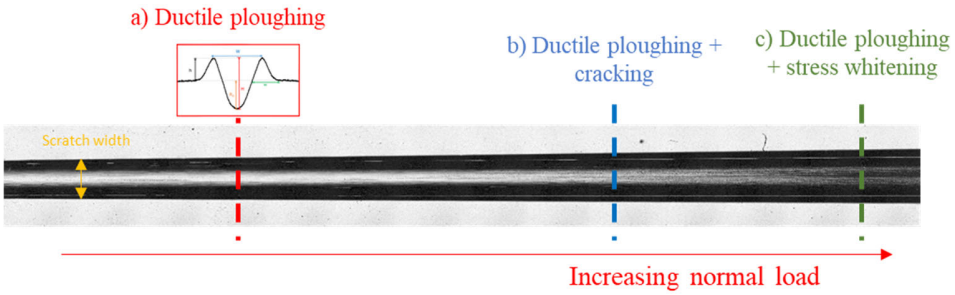

Figure 15.Scratch path is shown in the image: applied normal increases from left to right as well as the scratch width. Deformation mechanisms observed are: a) ductile ploughing, where materials pile-up along scratch edges, b) ductile ploughing and cracks formation are observed inside the scratch groove as a result of tensile stress building up beneath the indenter and as the load increases c) stress whitening and material removal inside the scratch groove.

3.5 Effect of physical aging on the scratch visibility

The scratch visibility was quantified with the automated SVA software and through a psychophysical test. The selected contrast threshold is 3.0%, which closely mimics the perception of the human eye, measured through the human eye assessment by asking at least five people to determine the onset of visibility. Figure 16 displays the variations of the critical load for the onset of visibility over the aging time measured through image analysis. Data were comparable to those obtained through human eye assessment. The critical load is increased for both PC and CoPC. The critical load is referred to as the load from which ductile ploughing begins to take place during scratching.

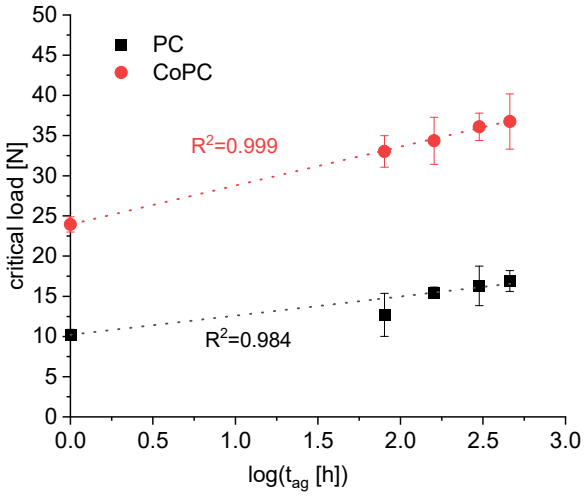

Figure 16. The graph shows the variation of the onset of visibility over the aging time. Both PC and PC copolymer show an increase of the critical load for the onset of visibility with the aging time.

The variation of the critical load for the onset of visibility with respect to the yield stress is shown in Figure 17. The critical load is strongly correlated with the increasing compressive yield stress. The increase of the yield stress leads to a lower scratch depth under a given applied stress, hence a lower component of the deformational frictional force for the tip to move ahead at a constant speed. This results in an increase of the critical load for the onset of visibility as the visibility is a geometrical phenomenon, originated by the formation of a groove in this case, mainly dependent on the scratch depth and on the height of the pile-up.

As a matter of fact, since the scratch deformation mechanisms and the aesthetic appearance (color and gloss) of the surface are the same, any difference in the scratch visibility must be ascribed to the scratch geometry, barring any effect of other surface optical properties such as color or microscopic roughness [24]. Figure 18 demonstrates how the scratch geometry at the onset of visibility, in terms of residual depth and shoulder height, does not significantly vary with the aging time, thus suggesting the existence of a critical level of deformation leading to scratch visibility. It would be interesting to verify this finding for other systems, investigating how this criterion depends on the characteristics of the original (i.e. unscratched) material. Another interesting aspect could be a quantitative description of the scratch geometry performed by evaluating the local surface orientation, as performed in [68, 69].

A monotonically increasing relationship between the critical load and compressive yield stress can be identified for PC and CoPC samples where the critical loads for scratch visibility correlate well with their respective yield stresses. The trend is quite interesting as it seems that by selecting a material with higher compressive yield stress, the critical load for onset visibility would also be increased – provided there is no change in the active scratching mechanisms (ductile ploughing). In this sense, it would also be intriguing to study the behavior at a shorter aging time to gain deeper understanding on the relationship between the critical load for visibility and polymer mechanical behavior. In any case, scratch visibility varies with aging time, being less susceptible to scratches with increasing aging time due mainly to their increased compressive yield stress. Also, it appears that the two materials show the same trend, and data lie on the same curve as shown by the red line in Figure 17. This should mean that the relationship between yield stress and critical load for onset of visibility is independent of the specific material, at least within a given family. It would be interesting to expand the array of selected materials for study, for instance, selecting semi-crystalline polymers, to validate this relationship. For the above relationship to remain valid, it is worth stating that the deformation mechanism responsible for the observed visibility should be consistent, i.e., materials must show ductile ploughing. This work will be addressed in our future research.

It was shown elsewhere [1], [7], [14], [26] that polymer scratch resistance, expressed in terms of scratch hardness, i.e., applied normal load over the projected contact area between indenter and material, is linearly increasing with compressive yield stress, the former being 1.54 - 1.80 times larger than the latter [14], [26], [2]. In the present work, the critical load for the onset of visibility is also linearly related to the compressive yield stress, which implies scratch visibility may be improved by tailoring the mechanical properties of polymers. It is interesting that scratch visibility is caused by the groove formation, which in turn is dominated by compressive yielding. It should be noted that the scratch hardness term cannot be a universal parameter that relates to scratch performance for two simple reasons. For one, polymers are viscoelastic in nature. Soft polymers, which have low scratch hardness values, may be able to easily recover after scratch. This recovery may change scratch profile, i.e., its visibility. As a matter of fact, a softer polymer may show a larger viscoelastic deformation upon scratching, but may recover its deformation more so than a rigid polymer with time. Similarly, some polymers may have similar modulus values but significantly different viscoelastic behavior; the polymer that can undergo more viscoelastic recovery will exhibit better scratch visibility resistance.

In any case, the above findings have a significant impact when it comes to the design of polymers for scratch resistant application, specifically in terms of scratch visibility, which represents the novelty of the present work. Also, it would allow to predict how the material may behave in the real-life application. However, this correlation may not be valid under different circumstances, such as longer aging time, use of another indenter geometry, different temperature and sliding velocity, etc. This implies that what has been shown is valid under specific conditions. If these conditions are not met, material may experience different deformation mechanisms and visibility can no longer be related to material yielding only.

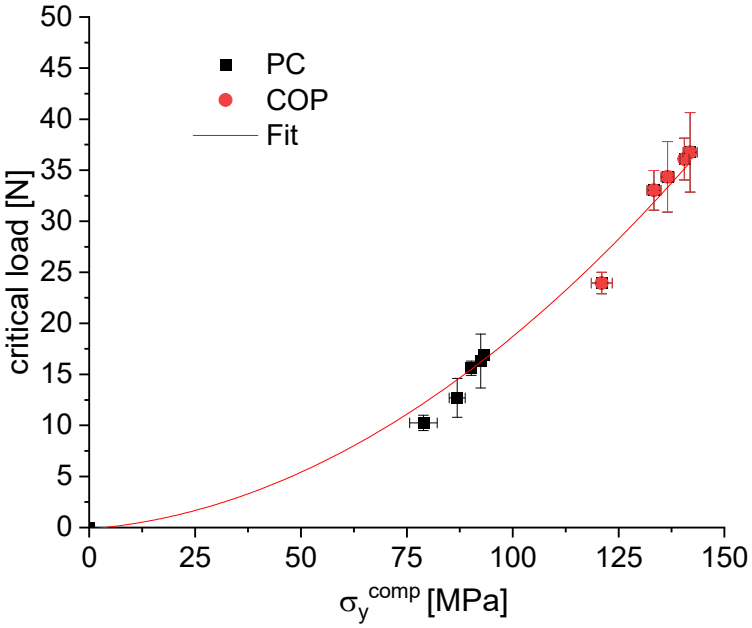

Figure 17. Variations of the critical load vs the compressive yield stress for PC (solid black squares) and PC copolymer (solid red circles). Solid red line shows data interpolation.

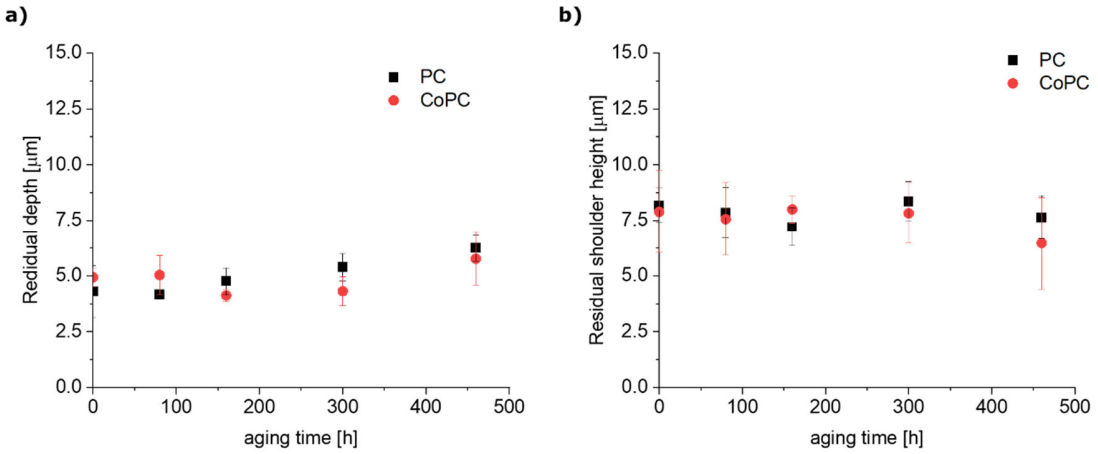

Figure 18. Scratch geometry at the onset of visibility for both PC and PC copolymer: a) residual depth and b) shoulder height (related to pile-up at the edges of the groove).

4 Conclusions

Physical aging was studied with the aim of investigating polymeric component durability against scratch damage over the aging time. Physical aging significantly affects polycarbonate scratch behavior:

- Critical load for the onset of visibility increases over the aging time, thus improving the scratch resistance in terms of visibility.
- A monotonically increasing relationship exists between the material compressive yield stress and the critical load for visibility. It is worth noting that scratch deformation mechanism does not vary over the aging time, thus this relationship holds true for each aging time investigated in this study. Both polycarbonate and polycarbonate copolymer show the same trends. Therefore, the present study suggests that it is possible to rank materials' scratch performance according to their compressive yield stress if the dominant mode of deformation is ductile ploughing. It would also be interesting to carry out the same experimental procedure on other materials to strengthen the observed relationship.
- It is worth pointing out that different scratch deformation mechanisms may lead to different critical load trends. For instance, if the material deformation involves a significant viscoelastic contribution [67], which may significantly impact the residual scratch geometry without modifying the deformation mechanism. At the same time, if the scratch visibility is caused by a different deformation mechanism, such as cracking or a roughening of the surface, then the ultimate tensile strength may be possibly considered as a dominant parameter to correlate with such phenomena. This topic could be addressed in future researches.
- These findings can be instrumental to show the relationship between polymer mechanical properties and scratch visibility, allowing to tailor polymer composition aiming at improving scratch resistance in terms of visibility. This also allows an estimate of the effect of physical aging on scratch resistance during the polymeric component lifetime.
- This study shows that PC scratch response improves with aging time, thus being more sustainable. This could also improve the existing model to better predict scratch resistance.

5 Acknowledgments

The authors would like to acknowledge the support of SABIC's Specialties business, the Texas A&M Scratch Behavior Consortium and BM Plastic (Italy). The authors especially want to thank BM plastic for sponsoring the PhD grant of Lorenzo De Noni.

References

[1] C. Xiang, H.-J. Sue, J. Chu, and B. Coleman, "Scratch behavior and material property relationship in polymers," *J. Polym. Sci. B Polym. Phys.*, vol. 39, no. 1, pp. 47–59, Jan. 2001, doi: 10.1002/1099-0488(20010101)39:1<47::AID-POLB50>3.0.CO;2-2.

[2] C. Gauthier and R. Schirrer, "Time and temperature dependence of the scratch properties of poly(methylmethacrylate) surfaces," p. 10.

[3] S. Lafaye, C. Gauthier, and R. Schirrer, "A surface flow line model of a scratching tip: apparent and true local friction coefficients," *Tribology International*, vol. 38, no. 2, pp. 113–127, Feb. 2005, doi: 10.1016/j.triboint.2004.06.006.

[4] V. Jardret and P. Morel, "Viscoelastic effects on the scratch resistance of polymers: relationship between mechanical properties and scratch properties at various temperatures," *Progress in Organic Coatings*, vol. 48, no. 2–4, pp. 322–331, Dec. 2003, doi: 10.1016/j.porgcoat.2003.02.002.

[5] J. L. Bucaille, C. Gauthier, E. Felder, and R. Schirrer, "The influence of strain hardening of polymers on the piling-up phenomenon in scratch tests: Experiments and numerical modelling," *Wear*, vol. 260, no. 7–8, pp. 803–814, Apr. 2006, doi: 10.1016/j.wear.2005.04.007.

[6] H. Jiang, G. T. Lim, J. N. Reddy, J. D. Whitcomb, and H.-J. Sue, "Finite element method parametric study on scratch behavior of polymers," *J. Polym. Sci. B Polym. Phys.*, vol. 45, no. 12, pp. 1435–1447, Jun. 2007, doi: 10.1002/polb.21169.

[7] H. Pelletier, C. Mendibide, and A. Riche, "Mechanical characterization of polymeric films using depth-sensing instrument: Correlation between viscoelastic-plastic properties and scratch resistance," *Progress in Organic Coatings*, vol. 62, no. 2, pp. 162–178, Apr. 2008, doi: 10.1016/j.porgcoat.2007.10.009.

[8] R. L. Browning, H. Jiang, and H.-J. Sue, "Scratch behavior of polymeric materials," in *Tribology and Interface Engineering Series*, Elsevier, 2008, pp. 354–373. doi: 10.1016/S1572-3364(08)55015-4.

[9] H. Jiang, R. Browning, and H.-J. Sue, "Understanding of scratch-induced damage mechanisms in polymers," *Polymer*, vol. 50, no. 16, pp. 4056–4065, Jul. 2009, doi: 10.1016/j.polymer.2009.06.061.

[10] J.-I. Weon, S.-Y. Song, K.-Y. Choi, S.-G. Lee, and J. H. Lee, "Quantitative determination of scratch-induced damage visibility on polymer surfaces," *J Mater Sci*, vol. 45, no. 10, pp. 2649–2654, May 2010, doi: 10.1007/s10853-010-4243-8.

[11] J.-I. Weon *et al.*, "Quantitative evaluation of scratch-induced damage on polymer surfaces using a colorimetric analysis," *Macromol. Res.*, vol. 18, no. 6, pp. 610–613, Jun. 2010, doi: 10.1007/s13233-010-0606-x.

[12] H. Pelletier, J. Krier, and C. Gauthier, "Influence of local friction coefficient and strain hardening on the scratch resistance of polymeric surfaces investigated by finite element modeling," *Procedia Engineering*, vol. 10, pp. 1772–1778, 2011, doi: 10.1016/j.proeng.2011.04.295.

[13] K. Friedrich, H. J. Sue, P. Liu, and A. A. Almajid, "Scratch resistance of high performance polymers," *Tribology International*, vol. 44, no. 9, pp. 1032–1046, Aug. 2011, doi: 10.1016/j.triboint.2011.04.008.

[14] P. Kurkcu, L. Andena, and A. Pavan, "An experimental investigation of the scratch behaviour of polymers: 1. Influence of rate-dependent bulk mechanical properties," *Wear*, vol. 290–291, pp. 86–93, Jun. 2012, doi: 10.1016/j.wear.2012.05.005.

[15] Y.-L. Liang, E. Moghbelli, H.-J. Sue, R. Minkwitz, and R. Stark, "Effect of high temperature annealing on scratch behavior of acrylonitrile styrene acrylate copolymers," *Polymer*, vol. 53, no. 2, pp. 604–612, Jan. 2012, doi: 10.1016/j.polymer.2011.11.034.

[16] P. Kurkcu, L. Andena, and A. Pavan, "An experimental investigation of the scratch behaviour of polymers – 2: Influence of hard or soft fillers," *Wear*, vol. 317, no. 1–2, pp. 277–290, Sep. 2014, doi: 10.1016/j.wear.2014.03.011.

[17] M. M. Hossain, R. Minkwitz, P. Charoensirisomboon, and H.-J. Sue, "Quantitative modeling of scratch-induced deformation in amorphous polymers," *Polymer*, vol. 55, no. 23, pp. 6152–6166, Nov. 2014, doi: 10.1016/j.polymer.2014.09.045.

[18] M. Hamdi and H.-J. Sue, “Effect of color, gloss, and surface texture perception on scratch and mar visibility in polymers,” *Materials & Design*, vol. 83, pp. 528–535, Oct. 2015, doi: 10.1016/j.matdes.2015.06.073.
[19] C. J. Barr, L. Wang, J. K. Coffey, A. Gidley, and F. Daver, “New technique for the quantification of scratch visibility on polymeric textured surfaces,” *Wear*, vol. 384–385, pp. 84–94, Aug. 2017, doi: 10.1016/j.wear.2017.05.007.
[20] C. J. Barr, L. Wang, J. K. Coffey, and F. Daver, “Influence of surface texturing on scratch/mar visibility for polymeric materials: a review,” *J Mater Sci*, vol. 52, no. 3, pp. 1221–1234, Feb. 2017, doi: 10.1007/s10853-016-0423-5.
[21] S. Tagliabue, L. Andena, A. Pavan, A. Marenghi, E. Testa, and R. Frassine, “Ageing in athletics tracks: A multi-technique experimental investigation,” *Polymer Testing*, vol. 69, pp. 293–301, Aug. 2018, doi: 10.1016/j.polymertesting.2018.05.029.
[22] P. Gamonal-Repiso, M. Sánchez-Soto, S. Santos-Pinto, and M. L. Maspoch, “Influence of topography on the scratch and mar visibility resistance of randomly micro-textured surfaces,” *Wear*, vol. 440–441, p. 203082, Dec. 2019, doi: 10.1016/j.wear.2019.203082.
[23] L. Andena, S. Tagliabue, A. Pavan, A. Marenghi, M. Testa, and R. Frassine, “Probing athletics tracks degradation using a microscratch technique,” *Polymer Testing*, vol. 89, p. 106602, Sep. 2020, doi: 10.1016/j.polymertesting.2020.106602.
[24] L. De Noni *et al.*, “Effect of color on scratch and mar visibility of polymers,” *J of Applied Polymer Sci*, Feb. 2023, doi: 10.1002/app.53699.
[25] K. Noh, J. Fincher, R. Mimms, and H.-J. Sue, “Effect of mold temperature and additive migration on scratch behavior of TPOs at elevated temperatures,” *Polymer*, vol. 223, p. 123709, May 2021, doi: 10.1016/j.polymer.2021.123709.
[26] L. Andena and G. Chiarot, “Scratch hardness as a quasi-intrinsic parameter to measure the scratch resistance of polymers,” *Wear*, vol. 514–515, p. 204562, Feb. 2023, doi: 10.1016/j.wear.2022.204562.
[27] J. Germann, T. Bensing, and M. Moneke, “Correlation between Scratch Behavior and Tensile Properties in Injection Molded and Extruded Polymers,” *Polymers*, vol. 14, no. 5, p. 1016, Mar. 2022, doi: 10.3390/polym14051016.
[28] J. L. Bucaille, E. Felder, and G. Hochstetter, “Mechanical analysis of the scratch test on elastic and perfectly plastic materials with the three-dimensional finite element modeling,” *Wear*, vol. 249, no. 5–6, pp. 422–432, Jun. 2001, doi: 10.1016/S0043-1648(01)00538-5.
[29] R. S. Hadal and R. D. K. Misra, “Scratch deformation behavior of thermoplastic materials with significant differences in ductility,” *Materials Science and Engineering: A*, vol. 398, no. 1–2, pp. 252–261, May 2005, doi: 10.1016/j.msea.2005.03.028.
[30] A. Krupička, M. Johansson, and A. Hult, “Use and interpretation of scratch tests on ductile polymer coatings,” *Progress in Organic Coatings*, vol. 46, no. 1, pp. 32–48, Jan. 2003, doi: 10.1016/S0300-9440(02)00184-4.
[31] D. Saviello, L. Andena, D. Gastaldi, L. Toniolo, and S. Goidanich, “Multi-analytical approach for the morphological molecular and mechanical.” Journal of Applied Polymer Science, 2018.
[32] J. M. Hutchinson, “Physical ageing of polymers,” Progress in polymer science, 1995.
[33] L. C. E. Struik, *Physical ageing in amorphous polymers and other materials*. 1977.
[34] I. M. Hodge, “Physical Aging in Polymer Glasses,” *Science*, vol. 267, no. 5206, pp. 1945–1947, Mar. 1995, doi: 10.1126/science.267.5206.1945.
[35] L. C. Brinson and T. S. Gates, “Effects of physical aging on long term creep of polymers and polymer matrix composites,” *International Journal of Solids and Structures*, vol. 32, no. 6–7, pp. 827–846, Mar. 1995, doi: 10.1016/0020-7683(94)00163-Q.
[36] D. Cangialosi, V. M. Boucher, A. Alegría, and J. Colmenero, “Physical aging in polymers and polymer nanocomposites: recent results and open questions,” *Soft Matter*, vol. 9, no. 36, p. 8619, 2013, doi: 10.1039/c3sm51077h.

[37] A. J. Kovacs, J. J. Aklonis, J. M. Hutchinson, and A. R. Ramos, “Isobaric volume and enthalpy recovery of glasses. II. A transparent multiparameter theory,” *J. Polym. Sci. Polym. Phys. Ed.*, vol. 17, no. 7, pp. 1097–1162, Jul. 1979, doi: 10.1002/pol.1979.180170701.
[38] J. M. G. Cowie and R. Ferguson, “Physical aging studies in poly(vinylmethyl ether). I. Enthalpy relaxation as a function of aging temperature,” *Macromolecules*, vol. 22, no. 5, pp. 2307–2312, May 1989, doi: 10.1021/ma00195a053.
[39] H. Cai, V. Dave, R. A. Gross, and S. P. McCarthy, “Effects of physical aging, crystallinity, and orientation on the enzymatic degradation of poly(lactic acid),” *J. Polym. Sci. B Polym. Phys.*, vol. 34, no. 16, pp. 2701–2708, Nov. 1996, doi: 10.1002/(SICI)1099-0488(19961130)34:16<2701::AID-POLB2>3.0.CO;2-S.
[40] S. Montserrat, “Physical aging studies in epoxy resins. I. Kinetics of the enthalpy relaxation process in a fully cured epoxy resin,” *J. Polym. Sci. B Polym. Phys.*, vol. 32, no. 3, pp. 509–522, Feb. 1994, doi: 10.1002/polb.1994.090320312.
[41] H. Wang, X. Sun, and P. Seib, “Properties of poly(lactic acid) blends with various starches as affected by physical aging,” *J. Appl. Polym. Sci.*, vol. 90, no. 13, pp. 3683–3689, Dec. 2003, doi: 10.1002/app.13001.
[42] G. B. McKenna, Y. Leterrier, and C. R. Schultheisz, “The evolution of material properties during physical aging,” *Polym. Eng. Sci.*, vol. 35, no. 5, pp. 403–410, Mar. 1995, doi: 10.1002/pen.760350505.
[43] W. H. Jo and K. J. Ko, “The effects of physical aging on the thermal and mechanical properties of an epoxy polymer,” *Polym. Eng. Sci.*, vol. 31, no. 4, pp. 239–244, Feb. 1991, doi: 10.1002/pen.760310406.
[44] G. M. Odegard and A. Bandyopadhyay, “Physical aging of epoxy polymers and their composites,” *J. Polym. Sci. B Polym. Phys.*, vol. 49, no. 24, pp. 1695–1716, Dec. 2011, doi: 10.1002/polb.22384.
[45] N. Yarahmadi, I. Jakubowicz, and T. Hjertberg, “The effects of heat treatment and ageing on the mechanical properties of rigid PVC,” *Polymer Degradation and Stability*, vol. 82, no. 1, pp. 59–72, Jan. 2003, doi: 10.1016/S0141-3910(03)00163-0.
[46] C. H. Ho and T. Vu-Khanh, “Physical aging and time–temperature behavior concerning fracture performance of polycarbonate,” *Theoretical and Applied Fracture Mechanics*, vol. 41, no. 1–3, pp. 103–114, Apr. 2004, doi: 10.1016/j.tafmec.2003.11.008.
[47] C. Ho Huu and T. Vu-Khanh, “Effects of physical aging on yielding kinetics of polycarbonate,” *Theoretical and Applied Fracture Mechanics*, vol. 40, no. 1, pp. 75–83, Jul. 2003, doi: 10.1016/S0167-8442(03)00035-1.
[48] V. A. Soloukhin, J. C. M. Brokken-Zijp, O. L. J. van Asselen, and G. de With, “Physical Aging of Polycarbonate: Elastic Modulus, Hardness, Creep, Endothermic Peak, Molecular Weight Distribution, and Infrared Data,” *Macromolecules*, vol. 36, no. 20, pp. 7585–7597, Oct. 2003, doi: 10.1021/ma0342980.
[49] A. J. Hill, K. J. Heater, and C. M. Agrawal, “The effects of physical aging in polycarbonate,” *J. Polym. Sci. B Polym. Phys.*, vol. 28, no. 3, pp. 387–405, Feb. 1990, doi: 10.1002/polb.1990.090280310.
[50] C. H. Ho and T. Vu-Khanh, “Effects of time and temperature on physical aging of polycarbonate,” *Theoretical and Applied Fracture Mechanics*, vol. 39, no. 2, pp. 107–116, Mar. 2003, doi: 10.1016/S0167-8442(02)00151-9.
[51] L. Guerdoux, R. A. Duckett, and D. Froelich, “Physical ageing of polycarbonate and PMMA by dynamic mechanical measurements,” *Polymer*, vol. 25, no. 10, pp. 1392–1396, Oct. 1984, doi: 10.1016/0032-3861(84)90098-3.
[52] S. Kahlen, G. M. Wallner, and R. W. Lang, “Aging behavior and lifetime modeling for polycarbonate,” *Solar Energy*, vol. 84, no. 5, pp. 755–762, May 2010, doi: 10.1016/j.solener.2010.01.021.

[53] J. M. Hutchinson, S. Smith, B. Horne, and G. M. Gourlay, “Physical Aging of Polycarbonate: Enthalpy Relaxation, Creep Response, and Yielding Behavior,” *Macromolecules*, vol. 32, no. 15, pp. 5046–5061, Jul. 1999, doi: 10.1021/ma981391t.
[54] A. Ohara and H. Kodama, “Correlation between enthalpy relaxation and mechanical response on physical aging of polycarbonate in relation to the effect of molecular weight on ductile-brittle transition,” *Polymer*, vol. 181, p. 121720, Oct. 2019, doi: 10.1016/j.polymer.2019.121720.
[55] D. J. A. Senden, J. A. W. van Dommelen, and L. E. Govaert, “Physical aging and deformation kinetics of polycarbonate,” *J. Polym. Sci. B Polym. Phys.*, vol. 50, no. 22, pp. 1589–1596, Nov. 2012, doi: 10.1002/polb.23161.
[56] Cheng, Q., Jiang, C., Zhang, J., Yang, Z., Zhu, Z., & Jiang, H. (2016). Effect of thermal aging on the scratch behavior of poly (methyl methacrylate). Tribology International, 101, 110-114.

[57] Zhu, Z., Cheng, Q., Jiang, C., Zhang, J., & Jiang, H. (2016). Scratch behavior of the aged hydrogenated nitrile butadiene rubber. Wear, 352, 155-159.

[58] van Breemen L. C. A., *Contact mechanics in glassy polymers*. Technische Universiteit Eindhoven, 2009.
[59] H. G. H. van Melick, L. E. Govaert, B. Raas, W. J. Nauta, and H. E. H. Meijer, “Kinetics of ageing and re-embrittlement of mechanically rejuvenated polystyrene,” *Polymer*, vol. 44, no. 4, pp. 1171–1179, Feb. 2003, doi: 10.1016/S0032-3861(02)00863-7.
[60] A. L. Volynskii, A. V. Efimov, and N. F. Bakeev, “Structural aspects of physical aging of polymer glasses,” *Polym. Sci. Ser. C*, vol. 49, no. 4, pp. 301–320, Dec. 2007, doi: 10.1134/S1811238207040017.
[61] M. Hamdi, D. Manica, and H.-J. Sue, “A Multidimensional Scaling Analysis of Surface Perceptual Parameters on Scratch and Mar Visibility Resistance in Polymers,” *SAE Int. J. Mater. Manf.*, vol. 10, no. 2, pp. 94–106, Apr. 2017, doi: 10.4271/2017-01-9451.
[62] J. Chrisman, S. Xiao, M. Hamdi, H. Pham, M. J. Mullins, and H.-J. Sue, “Testing and evaluation of mar visibility resistance for polymer films,” *Polymer Testing*, vol. 69, pp. 238–244, Aug. 2018, doi: 10.1016/j.polymertesting.2018.05.011.
[63] E. Peli, “Contrast in complex images,” *J. Opt. Soc. Am. A*, vol. 7, no. 10, p. 2032, Oct. 1990, doi: 10.1364/JOSAA.7.002032.
[64] A. A. Michelson, *Studies in optics*, 1. publ. in Dover books on physics. New York: Dover Publications, 1995.
[65] H. Jiang, R. Browning, J. Fincher, A. Gasbarro, S. Jones, and H.-J. Sue, “Influence of surface roughness and contact load on friction coefficient and scratch behavior of thermoplastic olefins,” *Applied Surface Science*, vol. 254, no. 15, pp. 4494–4499, May 2008, doi: 10.1016/j.apsusc.2008.01.067.
[66] E. Amerio, P. Fabbri, G. Malucelli, M. Messori, M. Sangermano, and R. Taurino, “Scratch resistance of nano-silica reinforced acrylic coatings,” *Progress in Organic Coatings*, vol. 62, no. 2, pp. 129–133, Apr. 2008, doi: 10.1016/j.porgcoat.2007.10.003.
[67] G. Molero *et al.*, “Mechanical and scratch behaviors of polyrotaxane-modified poly(methyl methacrylate).” Journal of Applied Polymer Science, 2021.
[68] Wittmann, B., Montmitonnet, P., Gauthier, C., Burr, A., Agassant, J. F., Favier, D., & Casoli, A. (2023). Analysis of scratch visibility on polymeric surfaces using 3D roughness measurement and the bidirectional reflectance distribution function (BRDF). *Progress in Organic Coatings*, *185*, 107935, doi: 10.1016/j.porgcoat.2023.107935

[69] Wittmann, B., Montmitonnet, P., Burr, A., Gauthier, C., Agassant, J. F., & Casoli, A. (2021). BRDF and gloss computation of polyurethane coatings from roughness measurements: modelling and experimental validation. *Progress in Organic Coatings*, *156*, 106247, doi: 10.1016/j.porgcoat.2021.106247